

# The $\alpha$ Subunit of Sea Urchin Sperm Outer Arm Dynein Mediates Structural and Rigor Binding to Microtubules

Anthony G. Moss, Winfield S. Sale,\* Laura A. Fox,\* and George B. Witman

Worcester Foundation for Experimental Biology, Shrewsbury, Massachusetts, 01545; and \*Department of Cell Biology and Anatomy, Emory University School of Medicine, Atlanta, Georgia 30322

**Abstract.** Glass-adsorbed intact sea urchin outer arm dynein and its  $\beta$ /IC1 subunit supports movement of microtubules, yet does not form a rigor complex upon depletion of ATP (16). We show here that rigor is a feature of the isolated intact outer arm, and that this property subfractionates with its  $\alpha$  heavy chain. Intact dynein mediates the formation of ATP-sensitive microtubule bundles, as does the purified  $\alpha$  heavy chain, indicating that both particles are capable of binding to microtubules in an ATP-sensitive manner. In contrast, the  $\beta$ /IC1 subunit does not bundle microtubules. Bundles formed with intact dynein are composed of ribbon-like sheets of parallel microtubules that are separated by 54 nm (center-to-center) and display the same longitudinal repeat (24 nm) and cross-sectional geometry of dynein arms as do outer doublets in situ. Bundles formed by the  $\alpha$  heavy chain are composed of microtubules with a center-to-center

spacing of 43 nm and display infrequent, fine cross-bridges. In contrast to the bridges formed by the intact arm, the links formed by the  $\alpha$  subunit are irregularly spaced, suggesting that binding of the  $\alpha$  heavy chain to the microtubules is not cooperative. Cosedimentation studies showed that: (a) some of the intact dynein binds in an ATP-dependent manner and some binds in an ATP-independent manner; (b) the  $\beta$ /IC1 subunit does not cosediment with microtubules under any conditions; and (c) the  $\alpha$  heavy chain cosediments with microtubules in the absence or presence of  $MgATP^{2-}$ . These results suggest that the structural binding observed in the intact arm also is a property of its  $\alpha$  heavy chain. We conclude that whereas force-generation is a function of the  $\beta$ /IC1 subunit, both structural and ATP-sensitive (rigor) binding of the arm to the microtubule are mediated by the  $\alpha$  subunit.

THE "A-end" of the outer dynein arm of ciliary and flagellar axonemes is permanently attached to the A-tubule of one outer doublet microtubule, while the "B-end" of the arm extends toward the B-tubule of the opposing outer doublet and is believed to transiently bind to and release that microtubule during ATP hydrolysis and force production (33). Biochemically, the outer arm consists of two or three subunits ( $\alpha$ ,  $\beta$ , and sometimes  $\gamma$ ), depending on species, each of which is organized around  $\alpha$  and  $\beta$  (and sometimes  $\gamma$ ) heavy chains (34, 36). The intact arm also contains two or more intermediate chains (ICs)<sup>1</sup> and several light chains (LCs). Each subunit exhibits ATPase activity, and although the subunits differ in their enzymatic properties, it is not known if they have different roles in the production of flagellar movement.

In studies of force production by the  $\beta$ /IC1 subunit of outer arm dynein isolated from sea urchin sperm flagella, we observed that the glass-adsorbed  $\beta$ /IC1 subunit was capable of

force production, but it did not form a "rigor" bond to microtubules in the absence of ATP (16). The  $\beta$ /IC1 subunit also did not form rigor or ATP-insensitive structural bonds in solution. The intact outer arm dynein similarly did not form rigor bonds when adsorbed to glass, although in solution it was capable of binding to microtubules. These observations led us to investigate ATP-sensitive and -insensitive microtubule binding by the intact arm and its individual subunits more closely. We report here that the motility-competent intact arm, as expected, is capable of both structural and rigor binding, and we confirm that the isolated  $\beta$ /IC1 subunit generates force but does not form structural or rigor bonds. In contrast, the isolated  $\alpha$  subunit retains the ability to form both types of bonds, but apparently does not generate force. Therefore, there appears to be a segregation of function between these two subunits.

## Materials and Methods

### Isolation of Dynein and Dynein Subunits

Dynein was extracted from isolated *Strongylocentrotus purpuratus* sperm tails by treatment with 0.6 M NaCl as described previously (16, 20). For

Address all correspondence to Dr. Witman.

1. Abbreviations used in this paper: IC, intermediate chain; LC, light chain.

some experiments, the 0.6 M NaCl extract was dialyzed into motility buffer (see below) and used as "crude dynein" without further purification. The intact outer arm was purified by centrifugation in sucrose density gradients containing 200 mM NaCl (16). The  $\alpha$  and  $\beta$ /IC1 subunits were dissociated from each other by dialysis of the 0.6 M NaCl extract into 5 mM Hepes/NaOH, pH 7.0, 0.5 mM EDTA (sometimes containing 1 or 2 mM *n*-Octyl  $\beta$ -D-glucopyranoside to reduce aggregation of the  $\alpha$  subunit), and the subunits purified by ultracentrifugation through a 5–20% sucrose gradient in the same buffer at pH 7.3. The fraction containing the  $\beta$ /IC1 peak was collected and dialyzed into motility buffer (see below) for use. Fractions 1–6 from the bottom of the gradient, containing virtually pure  $\alpha$  heavy chain, were pooled and concentrated by centrifugation in a Centricon-30 cell (Amicon Corp., Danvers, MA) for 15–60 min at 5,000 g (6,500 rpm) (SS-34 rotor; Sorvall, DuPont, Wilmington, DE); final concentration was typically 4–5 $\times$  original. In later trials we found that when fractions containing the  $\alpha$  heavy chain were pooled and dialyzed into the 0.6 M NaCl buffer used for the initial extraction, aggregation could be reduced further. These samples were subsequently dialyzed into motility buffer.

*Tetrahymena* 22S outer arm dynein (9) was generously provided by Dr. S. Marchese-Ragona (Pennsylvania State University, State College, PA).

Before use, all dynein preparations were dialyzed into motility buffer (10 mM Hepes/NaOH, pH 8.0, 4 mM MgSO<sub>4</sub>, 1 mM EGTA, 100 mM potassium acetate) in 12,000–14,000-molecular weight cutoff dialysis tubing (Spectra/Por 2; Spectrum Medical Ind., Inc., Los Angeles, CA) for 2–4 h at 4°C at a ratio of 1 sample/1,000 dialysis buffer (vol/vol). Without such dialysis, crude dynein and purified outer arm dynein did not exhibit microtubule binding or bundling, presumably because dynein-microtubule interactions are inhibited by high ionic strength (16).

Dynein fractions tended to contain aggregates which were visible as small spheres in the light microscope and evident as tangled amorphous material in negatively stained preparations examined by EM (not shown). Aggregates were removed from samples used for light microscopy and cosedimentation studies by centrifugation for 3 min at 134,000 g in an airfuge (95,000 rpm, A95 rotor; Beckman Instruments, Palo Alto, CA).

### Taxol-stabilized Microtubules

DEAE-purified calf brain tubulin (32) was thawed and polymerized by immersion of the vial in a 37°C water bath for 15 min. Microtubules were stabilized by addition of three volumes of 37°C motility buffer containing 120  $\mu$ M taxol (see reference 16), and allowed to incubate for an additional 30 min at 37°C, during which time the microtubules further lengthened. The microtubules, typically >20- $\mu$ m long, were washed by centrifugation in an airfuge (A95 rotor) for 5 min at 87,000 rpm and resuspended in 60  $\mu$ M taxol-containing motility buffer prior to use. Microtubules were stored at a stock concentration of 1–2 mg/ml tubulin, as determined by protein assay (3). The final concentration of microtubules was 100–200  $\mu$ g/ml in the motility assays and 0.5–1.25 mg/ml in the cosedimentation assays.

### Video Microscopy

Video-enhanced microscopy was performed on a Zeiss IM-35 (Carl Zeiss, Oberkochen, Germany) equipped with differential interference contrast (DIC) optics and high intensity light source as previously described (16).

### EM

Pellets of microtubules and microtubule bundles were fixed in 2% glutaraldehyde, 1% tannic acid, 10 mM sodium cacodylate buffer at pH 7.4 for 1 h on ice. Samples were subsequently rinsed in 10 mM sodium cacodylate for three 3-min exchanges, and postfixed in 1% OsO<sub>4</sub> for 30 min on ice. Samples were then held in 10 mM sodium cacodylate overnight for subsequent dehydration and embedding the next day. Alternatively, samples were fixed overnight on ice and subsequently processed as above for EM. Microtubule associations were studied throughout the depth of each pellet for each sample.

### Cosedimentation Assays

Cosedimentation assays were performed as follows: 10  $\mu$ l of taxol-stabilized microtubules, 0.5  $\mu$ l of 10 mM taxol in DMSO, and varying volumes of the dynein preparation and motility buffer were combined to a total of 100  $\mu$ l final volume. The dynein was allowed to bind to the microtubules for 30 min to 1 h at room temperature (21–23°C), at the end of which time the sample was centrifuged in an airfuge at 87,000 rpm (A95 rotor) or 93,000 rpm (A100 rotor) for 1.5 min, which is sufficient to pellet microtubules but

not soluble dynein. The resulting supernatant (S1), which contained unbound dynein, was carefully collected, and the pellet was resuspended in 100  $\mu$ l of 4 mM ATP-containing motility buffer, sometimes containing 10 mM phosphocreatine and 0.2 mg/ml phosphocreatine kinase to regenerate ATP from ADP produced as a result of ATP hydrolysis. This was allowed to incubate at room temperature for 2 min, and the sample was then centrifuged a second time for 1.5 min. The second supernatant (S2), containing dynein that was released from the microtubules by ATP, was separated from the pellet (P), which contained dynein bound to microtubules in an ATP-insensitive manner. All three samples were diluted into SDS gel sample buffer (14), boiled for 5 min, and then loaded on SDS-containing polyacrylamide gels. In some cases, the control consisted of sedimentation of the dynein in the absence of ATP. The supernatant was then called S; the pellet, P.

### Gel Electrophoresis

Polypeptide composition was assayed on discontinuous SDS-polyacrylamide gels (14). Coomassie brilliant blue-stained, 5–15% polyacrylamide linear gradient gels were used to routinely assay the purity of preparations, and to determine tubulin and dynein content of pellets and supernatants from cosedimentation experiments. Silver-stained (15), 5–17.5% polyacrylamide gradient gels were used to assay the polypeptide composition of outer arm dynein and to characterize the intermediate chain/light chain complex. 3–5% linear polyacrylamide gradient gels were used to resolve the  $\alpha$  and  $\beta$  dynein heavy chains. All gels were 15-cm long.

Masses of the polypeptides constituting the intact sea urchin outer arm were estimated by SDS-PAGE using the following standards: skeletal muscle myosin (205 kD),  $\beta$ -galactosidase (116 kD), phosphorylase b (97.4 kD), bovine serum albumin (66.2 kD), ovalbumin (45 kD), soybean trypsin inhibitor (21.5 kD), lysozyme (14.4 kD), aprotinin (6.5 kD), and insulin (2 and 3 kD). A curve of mass vs.  $R_f$  was generated and fitted by a fourth order polynomial of the form  $y = ax^0 + bx^1 + cx^2 + dx^3$  where  $x = R_f$ , using Sigma Plot (Jandel Scientific, CA). The mass of each unknown sea urchin polypeptide was determined by substitution of its  $R_f$  in the polynomial equation.

### Reagents

All reagents were as described in (16). Taxol was kindly provided by Ms. Nancita Lomax of the National Cancer Institute (National Institutes of Health, Bethesda, MD).

### Results

#### Composition of Sea Urchin Dynein Fractions

Fig. 1 illustrates typical protein and polypeptide profiles of the sucrose gradients used to isolate sea urchin dynein and dynein subunits for this study. As previously reported, *S. purpuratus* sperm outer arm dynein contains two heavy chains,  $\alpha$  and  $\beta$ , complexed with three ICs of 70, 79, and 112 kD (17, 21); it also contains six LCs of 6.4–23 kD not described previously (Fig. 1 B). The outer arm remained intact in sucrose gradients containing 200 mM KCl and migrated at  $\sim$ 21 S (Fig. 1, A and B).

Low ionic strength dialysis resulted in dissociation of the outer arm into several particles of consistent composition (Fig. 1, A and C) (22). The  $\beta$ /IC1 subunit, consisting of the  $\beta$  heavy chain and the 112 kD IC (IC1), migrated as a peak at  $\sim$ 11 S. The  $\alpha$  heavy chain migrated throughout the lower regions of the sucrose gradient, indicating that it was aggregated. A small but distinct peak, which migrated just ahead of the  $\beta$ /IC1 subunit (but more slowly than the intact dynein did in the sucrose gradients containing 200 mM KCl), consisted of the  $\alpha$  and  $\beta$  heavy chain and IC1. ICs 2 (79 kD) and 3 (70 kD) and the entire LC complement were missing from this peak. When this peak was collected and recentrifuged in a 600 mM KCl, 5–20% sucrose gradient, all three polypeptides again peaked in the same fractions

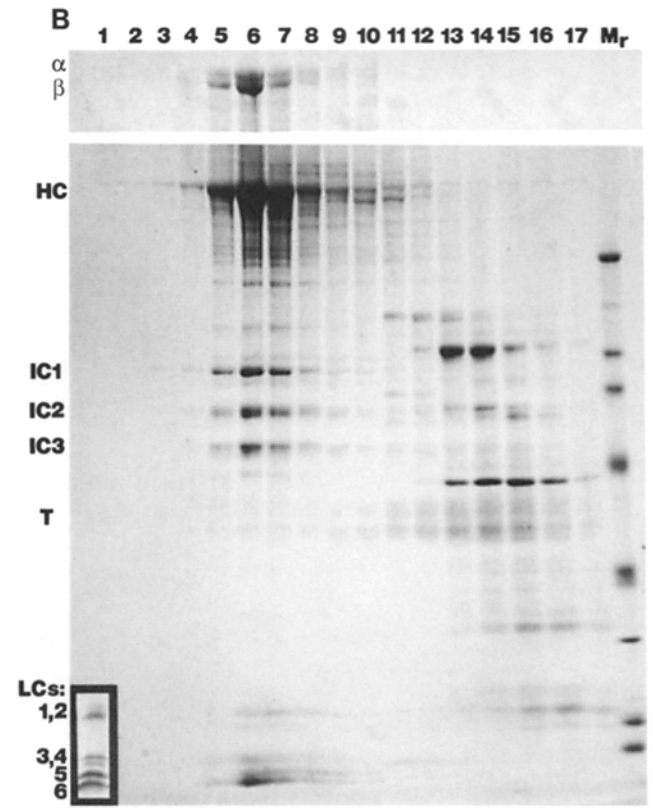
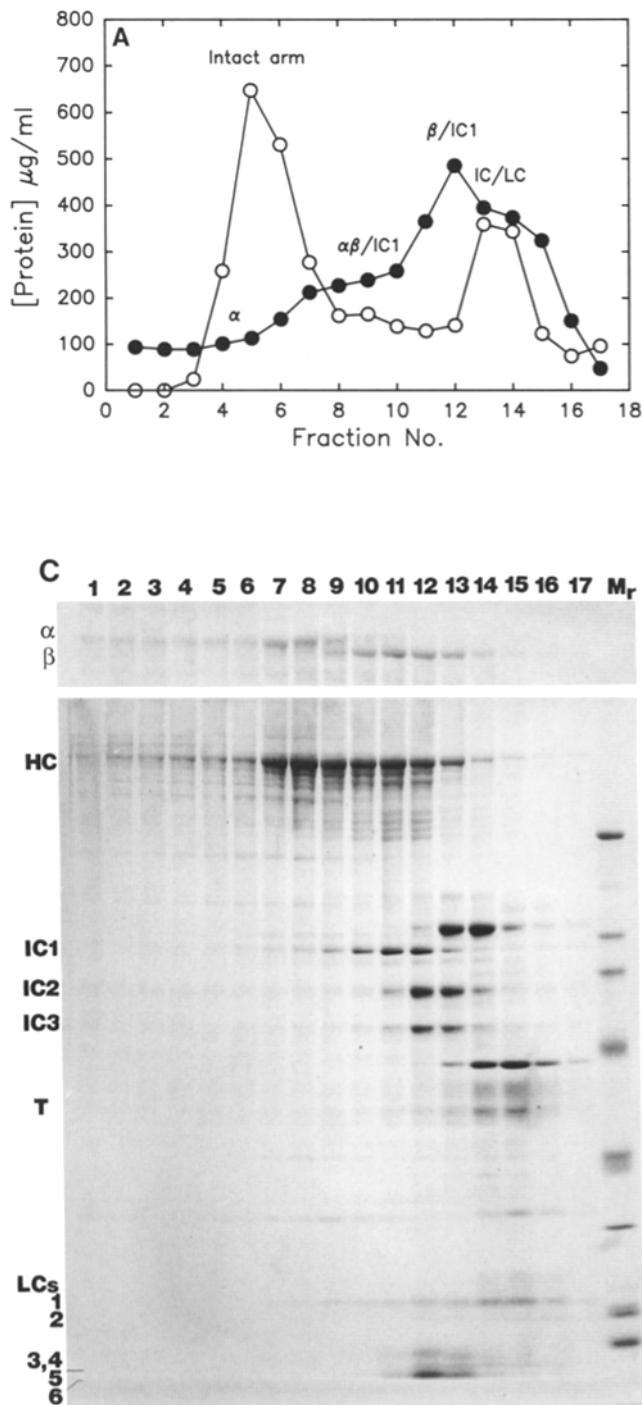


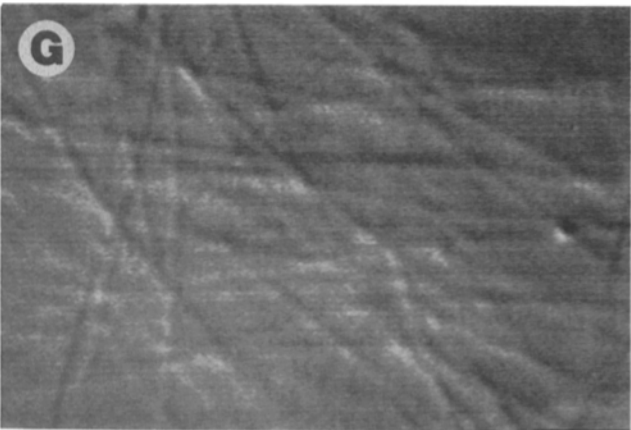
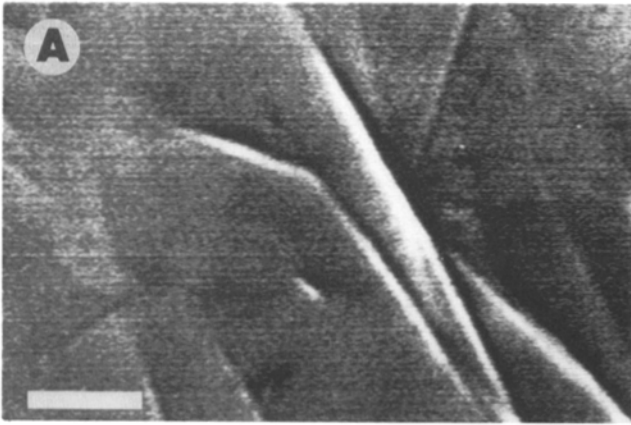
**Figure 1.** Polypeptide composition of the intact dynein and dynein subunits used in this study. (A) Protein profile of 5–20% linear sucrose gradients in 200 mM KCl (—○—) and low ionic strength buffer (—●—) used for purification of the intact outer arm dynein and outer arm subunits, respectively, from a high salt extract. Intact arm indicates position of the intact 21S dynein in the sucrose gradient containing 200 mM KCl;  $\alpha$ ,  $\alpha\beta$ /IC1,  $\beta$ /IC1, and IC/LC indicate positions of these complexes in the sucrose gradient made up in low ionic strength buffer. (B) SDS–polyacrylamide gels of the 200 mM salt sucrose gradient fractions shown in A. Above, heavy chain region of 3–5% acrylamide gradient gel; below, 5–15% acrylamide gradient gel.  $\alpha$  and  $\beta$  heavy chains ( $\alpha, \beta$ ) are resolved in the 3–5% gel but migrate as a single band (*H*) in the 5–15% gel. Intermediate chains (*IC*) 1, 2, and 3 and light chains (*LCs*) 1–6 are indicated; *T*: tubulin. Light chains 3 and 4 are not resolved in this gel, but are resolved in the inset, which shows the light chain region from another gel. (C) 3–5% (above) and 5–15% (below) SDS–polyacrylamide gel of the low ionic strength sucrose gradient fractions shown in A; format and key same as in B. Molecular weight standards ( $M_r$ ) top to bottom of gel (in kD): 200, 116.5, 97.4, 66.2, 45, 31, 21.5, 14.4. Coomassie brilliant blue stain, except for inset of B, which was silver stained.

(8–9), indicating that they were associated as an  $\alpha/\beta$ /IC1 complex (not shown).

Low ionic strength dialysis also consistently produced a distinct IC/LC complex that migrated slightly more slowly in the sucrose gradient than the  $\beta$ /IC1 subunit. This complex consisted of ICs 2 and 3 and at least LCs 1 (22.6 kD), 2 (20.8 kD), 3 (12.5 kD), 4 (9.7 kD), and 6 (6.4 kD). The relative intensities of light chains 1 and 2 varied considerably between preparations. LC 5 (7.5 kD) usually remained near the top of the gradient, but in some gradients its position overlapped that of the other light chains (Fig. 1 C), suggesting that it also may be a component of the IC/LC complex.

**Intact Outer Arm Dynein Bundles Microtubules in an ATP-sensitive Manner**

Microtubule bundling was used as a simple yet sensitive assay to investigate the ability of the soluble dynein to interact with microtubules in an ATP-dependent manner. When the dialyzed crude dynein or purified intact outer arm dynein was added to purified calf brain microtubules, the microtubules rapidly became linked together in large bundles (Fig. 2 A). These microtubule bundles, unlike individual microtubules, could be observed readily by light microscopy without image enhancement, as they were highly birefringent



structures which exhibited little thermal motion and formed a rigid, anastomosing network. Frequently, bundles were so extensive that they formed a gel which could trap small bubbles. Bundles not attached to the glass surface of the observation chamber were ATP sensitive, and promptly and completely fell apart when millimolar ATP was perfused into the observation chamber (Fig. 2 B). Bundles nearest the site of addition of the ATP-containing buffer, close to the edge of the coverslip, were completely dissociated by the time the preparation could be observed (within 30 s). Further from the site of ATP addition, bundles usually were observed to fall apart with a shaking movement. Only very rarely was disintegration by inter-microtubule sliding clearly observed. In one case, a microtubule was observed to cyclically loop out from a bundle of microtubules and then collapse back into the bundle (not shown); we calculated that this microtubule was sliding at a rate of about 6  $\mu\text{m/s}$ , comparable to the rates observed for microtubules moving on glass-adsorbed intact dynein (16). Microtubules released from the bundles frequently attached to the glass surface of the chamber and were translocated over the surface, indicating that dynein from the microtubule-dynein mixture (and/or released from the bundles) had adsorbed to the free glass surfaces and was capable of generating motility. These microtubules eventually released from the glass due to depletion of  $\text{MgATP}^{2-}$ , as described previously (16).

Bundles attached to the surface of the coverslip usually did not respond to ATP addition. They remained intact and continued to adhere to the glass in the presence or absence of ATP, despite thorough perfusion with several times the chamber volume of buffer, which was sufficient to wash out all microtubules in suspension. Such adherent bundles were observed even though individual microtubules were being actively translocated across the same glass surface (see above). Therefore, the bundles probably were attached directly to the glass.

#### ***The $\alpha$ Subunit, but not the $\beta/\text{IC1}$ Subunit, Produces ATP-sensitive Microtubule Bundles***

The purified  $\alpha$  subunit also bundled microtubules into large, highly birefringent arrays (Fig. 2 C). In the light microscope, these bundles appeared very similar to those formed by the crude dynein or intact outer arm, except that some of the bundles were more tangled. The  $\alpha$  subunit-induced bundles also fell apart into single microtubules upon addition of ATP (Fig. 2 D); this occurred without noticeable sliding movement of the microtubules. Microtubules that were released from the bundles occasionally bound to the surface of the observation chamber; these adherent microtubules were not translocated over the glass.

In contrast, the  $\beta/\text{IC1}$  subunit did not induce the formation of microtubule bundles in either the absence (Fig. 2 E) or presence of ATP (Fig. 2 F). When ATP was added to observation chambers previously loaded with microtubules and

the  $\beta/\text{IC1}$  subunit, individual microtubules became attached to the coverslip and were translocated over its surface, confirming that the  $\beta/\text{IC1}$  subunits in these preparations were functional. These microtubules eventually were released into suspension upon hydrolysis of ATP, as previously described (16).

#### ***The Intact Arm and the $\alpha$ Subunit, but not the $\beta/\text{IC1}$ Subunit or the IC/LC Complex, Cosediment with Microtubules***

The above observations of ATP-sensitive microtubule bundling by the intact sea urchin dynein and its  $\alpha$  subunit indicates that these particles can form a rigor bond with microtubules. Although bundling implies that a minimum of two bonds were formed per dynein, it is possible that the microtubules were cross-bridged by the two heads in the case of the intact arm, or by multiple heads in the case of the  $\alpha$  subunit, if the latter were aggregated by their stems. Therefore, to determine if bundling was mediated solely by rigor binding, or by a combination of structural and rigor binding, we investigated the abilities of the dynein and dynein subunits to cosediment with microtubules. Unbound dynein would be expected to remain in the S1 supernatant (see Materials and Methods). Dynein molecules attached to microtubules solely by rigor bonds would be expected to release completely upon application of ATP, and thus be recovered in the S2 supernatant. Finally, dynein that bundled microtubules by a combination of structural and rigor binding would be expected to remain attached to the microtubules by their A-ends even after dissociation of the bundles by ATP. In this case, the dynein would cosediment with the microtubules in the presence of ATP, and be recovered in the final pellet.

When crude dynein or the purified intact arm was mixed with microtubules in the absence of ATP, most of the dynein cosedimented with the microtubules. When the microtubules were resuspended in the presence of ATP, a variable but typically small proportion of the dynein was released into solution (Fig. 3 C, lane S2), indicating that some of the molecules probably were bound only by rigor bonds. The remainder of the dynein cosedimented with the microtubules in the presence of ATP (Fig. 3 C, lane P), indicating that these dyneins were bound by ATP-insensitive structural bonds. In control experiments, very little crude or intact dynein sedimented in the absence of microtubules (Fig. 3 C, lane P). If microtubules were added back to the dynein remaining in the S1 supernatant, the proportion of the residual dynein that bound to the microtubules was about the same as that observed for the total dynein (not shown), indicating that the partitioning of dynein into bound vs. unbound fractions reflected the equilibrium of binding rather than separation of the dynein into two populations with different affinities for microtubules. Variability in the proportion of dynein that was bound by its A-end vs. its B-end was probably due to several factors,

**Figure 2.** ATP-sensitive bundling of microtubules by intact sea urchin outer arm dynein and its  $\alpha$  heavy chain as recorded by video-enhanced DIC microscopy. (A) Sucrose-gradient purified intact outer arm dynein ("21S dynein") added to microtubules in the absence of ATP. (B) As in A, but with ATP added. (C)  $\alpha$  heavy chain added to microtubules in absence of ATP. (D) As in C, but with ATP added. (E)  $\beta/\text{IC1}$  added to microtubules in the absence of ATP. (F) As in E, but with ATP added. (G) Microtubules in the absence of dynein and ATP. ATP does not change their appearance. Bar, 2.5  $\mu\text{m}$ .

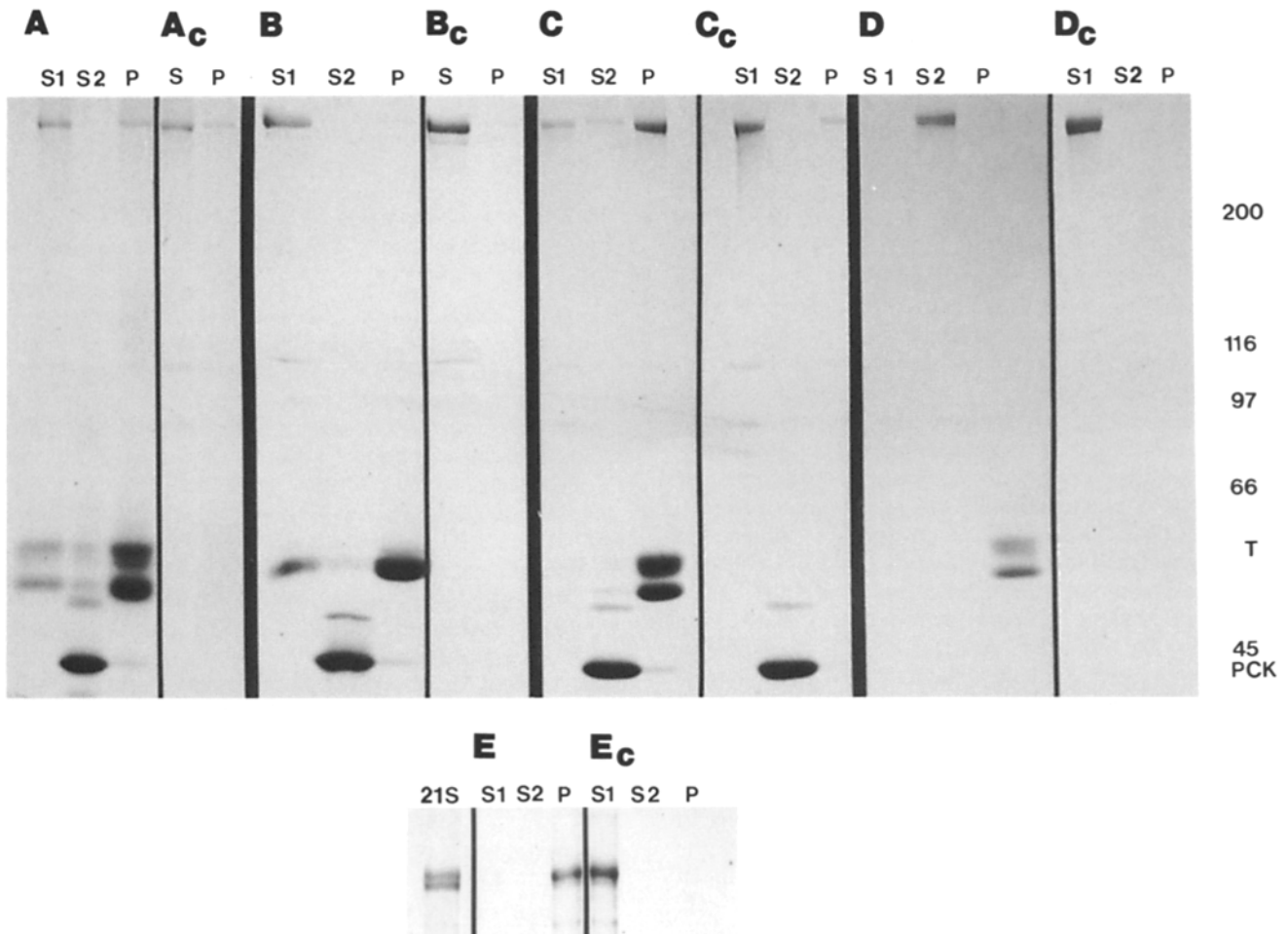


**Figure 3.** Cosedimentation of dynein with microtubules. Dynein was centrifuged in the presence (experimentals *A–E*) or absence (controls *A<sub>c</sub>–E<sub>c</sub>*) of microtubules. *A, A<sub>c</sub>, E, E<sub>c</sub>*, sea urchin dynein  $\alpha$  heavy chain. *B, B<sub>c</sub>*, sea urchin dynein  $\beta$ /IC1 subunit. *C, C<sub>c</sub>*, sucrose-gradient purified intact outer arm dynein from sea urchin sperm. *D, D<sub>c</sub>*, *Tetrahymena* intact outer arm dynein. *S1*, first supernatant, obtained in the absence of ATP. *S2*, supernatant obtained by resuspending first pellet in the presence of ATP followed by recentrifugation. *P*, pellet obtained from centrifugation in the presence of ATP. In controls, *S, P* indicate supernatant and pellet obtained by centrifugation in absence of ATP. *T*, tubulin; *PCK*, phosphocreatine kinase included to maintain ATP concentration. 5–15% polyacrylamide-SDS denaturing gels except for *E, E<sub>c</sub>*, which is a 3–5% gel; Coomassie Brilliant Blue stain, except for *E, E<sub>c</sub>*, which was silver-stained. In *E*, *21S* indicates a lane loaded with intact sea urchin outer arm dynein to mark the positions of the  $\alpha$  and  $\beta$  dynein heavy chains.

including the amount of free tubulin present in the preparations (7).

When the purified  $\alpha$  subunit was mixed with microtubules in the absence of ATP, a variable but significant proportion cosedimented with the microtubules (Fig. 3, *A* and *E*). No detectable quantity of this bound  $\alpha$  subunit was released by ATP. Often some of the  $\alpha$  subunit was recovered in the pellet even in the absence of microtubules, suggesting that it was still continuing to undergo aggregation (Fig. 3 *A<sub>c</sub>*, lane *P*). However, the amount of  $\alpha$  subunit recovered in the pellet was never as great in the absence of microtubules as in their presence. These results suggest that the  $\alpha$  subunit is capable of forming an ATP-insensitive structural bond with microtubules.

In contrast, the  $\beta$ /IC1 subunit never cosedimented with microtubules in either the presence or absence of ATP (Fig. 3 *B*).

Isolated IC/LC complexes also did not cosediment with microtubules in either the presence or absence of ATP (not

shown). Moreover, no binding or translocation of microtubules was observed in in vitro motility assays using the purified IC/LC complex. Thus, we did not obtain any evidence that this complex, as isolated, interacts directly with microtubules.

As an additional control, we examined the ability of *Tetrahymena* 22S outer arm dynein to cosediment with microtubules under our conditions. In agreement with the results of previous investigators (18), all of this dynein bound to the microtubules in the absence of ATP and the majority was released by addition of ATP (Fig. 3 *D*).

#### *EM of Sea Urchin Dynein-mediated Microtubule Bundles*

Microtubule bundles formed by intact dynein and dynein subunits were examined by thin-section EM. At high ratios of intact dynein to tubulin (molar ratio dynein/purified tubulin 1:5.25), virtually all microtubules in the pellet were deco-

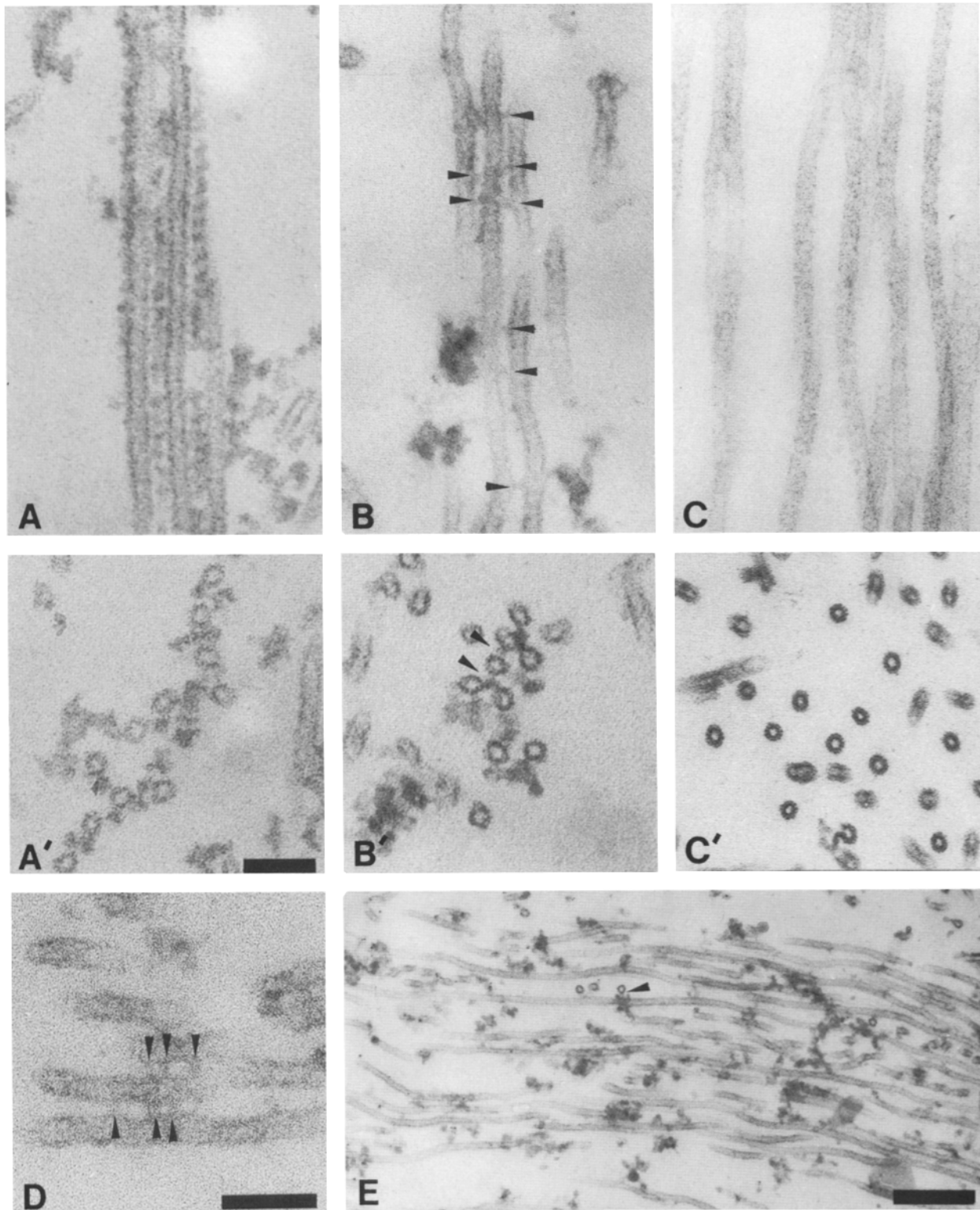


**Figure 4.** Thin-section electron micrographs of microtubules bundled by sucrose-gradient purified intact outer arm dynein (*A* and *A'*) and its  $\alpha$  heavy chain (*B*, *B'*, *D*, and *E*) in the absence of ATP. Arrowheads in *B*, *B'* and *D* indicate  $\alpha$  heavy chain crossbridges between microtubules. Arrowhead in *E* indicates where two microtubules crossing each other at right angles are cross-linked. *C* and *C'*, microtubules alone. Bars: (*A*-*D*) 0.1  $\mu\text{m}$ ; (*E*) 0.3  $\mu\text{m}$ .

rated. In longitudinal sections, microtubules were connected by bridges which exhibited a 24-nm repeat and closely resembled the outer arms seen between doublet microtubules in situ (5, 21, 28, 37, and see below) (Figs. 4, *A*, *A'*,

and 5, *A* and *B*). This is consistent with dynein binding to microtubules by both A- and B-ends. In cross-sections, pairs of microtubules held together by two rows of arms were frequently observed (*arrows*, Fig. 5 *A*). In addition, microtu-

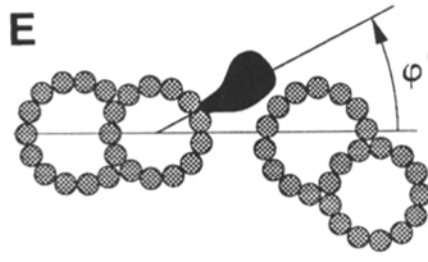
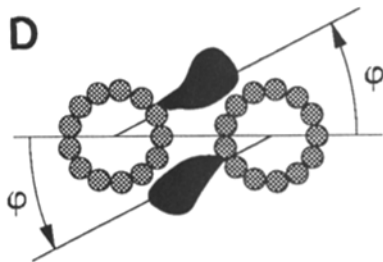
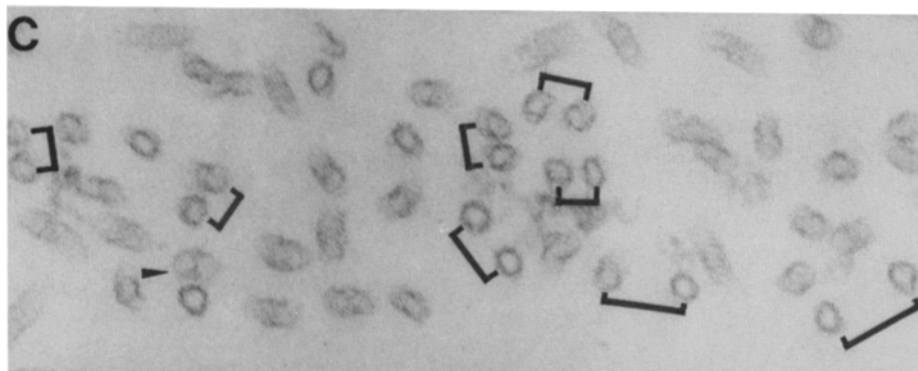
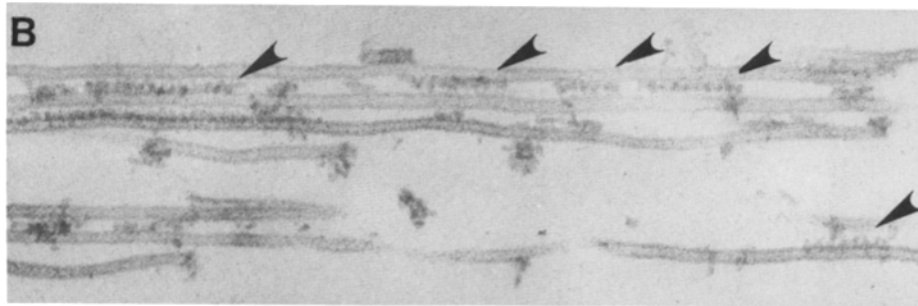
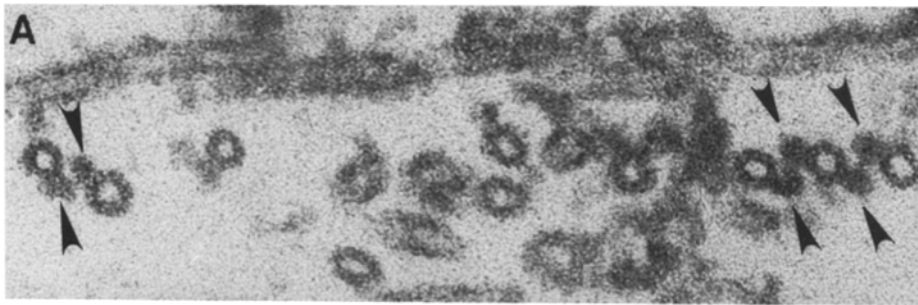


**Figure 5.** (A and B) Electron micrographs of taxol-stabilized brain microtubules bundled with intact dynein in the absence of ATP. Arrowheads in A indicate dynein arms; arrowheads in B indicate clusters of dynein arms bound to microtubules. (C) Microtubules without added dynein. Presumptive pairs of microtubules are marked by brackets. Arrowhead indicates a possible site of bifurcation. (D and E) Diagrams comparing the geometry of arms bound to taxol-stabilized microtubules in vitro (D) and to outer doublet microtubules in situ (E) ( $\phi$ ) Angle between one line running through the centers of the taxol-stabilized microtubules and a second line running through the axis of a bound arm; ( $\phi'$ ) Angle between one line running through the centers of A- and B-tubules of opposing outer doublet microtubules and a second line running through the axis of an arm in situ.

bules often were cross-linked into sheet-like bundles; in these cases the dynein-microtubule attachment points were located on opposite sides of any given microtubule (Figs. 4 A and 5 A). These sheets were either flat or rolled like a carpet. The sense of angular attachment of the dynein to the microtubules (5) indicated that all microtubules in a given bundle were of the same polarity. Intact dynein appeared to exhibit cooperativity in binding, because at lower dynein/tubulin ratios (1:75), the dynein bound in widely spaced clusters of 4–12 arms which still exhibited a 24-nm repeat

(Fig. 5 B). Such cooperativity has been reported previously for *Tetrahymena* (29) and *Chlamydomonas* (6) dyneins.

The presence of reciprocal bridges between pairs of microtubules raised the question of whether these microtubules were held together by dynein–dynein interactions, or by direct dynein–microtubule interactions at both ends of the arm. To investigate this, we compared the angle of attachment of such bridges with the angle of attachment of the outer arms in situ. The angle of attachment of the arms was in extraordinarily close agreement in the two cases: 27° for



the intact sea urchin axoneme, vs.  $28.8^\circ$  for the bundles formed in vitro (Fig. 5 D and E). Furthermore, the center-to-center spacing between the cross-bridged microtubules was the same (54 nm) as that of the A and B tubules of, respectively, the  $n$  and  $n + 1$  outer doublet microtubules in situ. These observations suggest that the two members of a pair of microtubules (see below) are kept parallel by direct dynein-microtubule interactions.

Bundles formed by the  $\alpha$  subunit also consisted of arrays of parallel microtubules (Fig. 4, B, D, and E), although the arrays were less well organized than those formed by the intact arm. The center-to-center spacing (43 nm) between microtubules in these bundles was  $\sim 20\%$  less than that in the bundles formed by the intact arm (c.f. Fig. 4, B' and A). Sometimes, a microtubule would appear to be attached to another microtubule at angles up to  $90^\circ$  (Fig. 4 E), suggesting that the  $\alpha$  heavy chain has considerable torsional flexibility; this was consistent with our light microscopic observations. In longitudinal sections (Fig. 4, B, D, and E), cross-bridges between the  $\alpha$  subunit-induced bundles were much less obvious than those in the bundles formed by the intact arm. However, close examination revealed fine links between the adjacent microtubules (arrows, Fig. 4, B and D). These cross-bridges usually were spaced irregularly along the microtubules. When viewed in cross-section, both ends of these bridges often appeared to intersect the walls of the microtubules at right angles (Fig. 4 B'); this is in contrast to the intact arm, in which the B-end always approaches a microtubule obliquely (see Figs. 4, A' and 5, A, C, and D).

In control preparations without dynein (Figs. 4, C and C' and Fig. 5 C), the pelleted microtubules usually were arranged parallel to one another over large areas, reflecting a long-range ordering due to steric hindrance (2, 8). Generally, the microtubules were not so closely packed as in the presence of dynein, and the spacing between tubules was less regular. However, these preparations also contained large numbers of paired, parallel microtubules (Fig. 1). The spacing between two members of a pair ranged from 0 nm (walls of the microtubules in contact) to tens of nanometers, beyond which distance it was uncertain whether the microtubules should be considered members of a pair. Such images suggested that the pairs represented microtubules diverging from a common source, most likely a bifurcated microtubule. These sections also revealed some S-shaped protofilament sheets as well as microtubules with associated protofilament hooks; these may represent intermediate structures in microtubule branching, growth, or depolymerization. Bridges were never observed between the paired or non-paired microtubules in control preparations.

## Discussion

### Segregation of Function between Dynein Subunits

In in vitro motility assays, the intact *S. purpuratus* outer arm dynein and its  $\beta$ /IC1 subunit were found to be capable of translocating microtubules, although neither subunit was observed to form a rigor bond to microtubules when adsorbed to a glass coverslip (16). We report here that the isolated outer arm dynein bundles microtubules in an ATP-sensitive manner, indicating that it is indeed capable of forming a rigor bond. Some of the bound dynein is released from the

microtubules by addition of ATP; the remainder cosediments with the microtubules even in the presence of ATP. Therefore, the isolated outer arm dynein also is able to form structural A-end bonds with microtubules.

To learn more about the specific roles of each subunit in the formation of rigor and structural bonds, the dynein was subfractionated into its  $\alpha$  and  $\beta$ /IC1 subunits, which were then tested individually for their ability to bundle microtubules or to cosediment with microtubules. The  $\beta$ /IC1 subunit did not bundle microtubules, nor did it cosediment with microtubules under any of the conditions tested. Therefore, although the isolated  $\beta$ /IC1 subunit retains the force-generating properties exhibited by the intact dynein (16), it does not exhibit the intact arm's ability to bind to microtubules in either an ATP-sensitive or an insensitive manner.

In contrast, the purified  $\alpha$  subunit bundled microtubules in an ATP-sensitive manner, indicating that it forms a rigor bond with microtubules. In addition, it cosedimented with microtubules in both the presence and absence of ATP, suggesting that it also attaches to microtubules by an ATP-insensitive structural bond. As with the intact arm, some of the  $\alpha$  subunit always failed to bind to the microtubules.

We cannot rule out the possibility that the subunits in situ have functional properties that were lost or masked during their isolation, or that simply were not revealed under our assay conditions. For example, the  $\alpha$  subunit may yet be demonstrated to be motile, and the  $\beta$ /IC1 subunit and/or the IC/LC complex may be involved in structural binding to microtubules (see reference 13). Nevertheless, all of the functional properties of the intact arm were recovered in one or the other of its subunits. Taken together, our observations suggest that these functional properties are segregated between the two subunits, with force generation being an attribute of the  $\beta$ /IC1 subunit, and rigor and structural binding being an attribute of the  $\alpha$  subunit.

### Implications for Dynein Arm Function In Situ

In the beating flagellum, axonemal bending occurs when the interdoubtlet shearing forces generated by the dynein arms are resisted by structures intrinsic to the axoneme (24). To generate and propagate coordinated bends, regions of resistance to interdoubtlet sliding, as well as regions of active and passive sliding (23, 25, 27), presumably must be carefully regulated in time, both around the circumference of the axoneme and along its length. The structures responsible for resisting interdoubtlet sliding have not yet been conclusively identified, but it has been suggested that the dynein arms themselves may function in this role (35). Perhaps rigor formation by the  $\alpha$  subunit actually represents a tight binding to microtubules that serves to limit interdoubtlet sliding and is controlled by ATP hydrolysis. In this case, the separate functions of "rigor" formation and force generation may be regulated more readily when they are segregated to different dynein subunits. As a result of a feedback loop monitoring some physical parameter associated with flagellar beating, one or the other of the dynein subunits might then be activated and so expressed in different regions of the axoneme at different times during the beat cycle. Although recent results have demonstrated that the  $\alpha$  heavy chain of the three-headed *Chlamydomonas* outer arm is not essential for flagellar movement (19), this chain may not be functionally

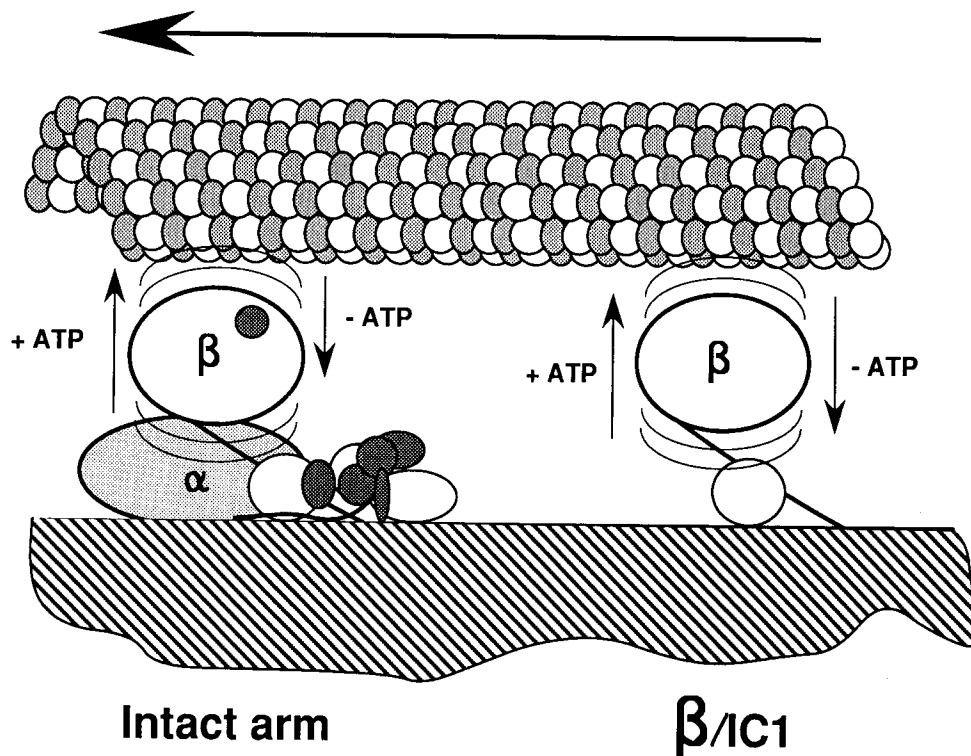


**Figure 6.** Model of intact outer arm dynein (*left*) and  $\beta$ /IC1 subunit interaction with microtubule in the *in vitro* motility assay. The  $\beta$ /IC1 subunit (*white*) is depicted as rapidly attaching to and detaching from the microtubule during the course of the ATP hydrolytic cycle. The  $\alpha$  heavy chain (*gray*) is not available to interact with the microtubule in the intact arm attached to glass. Positions of intermediate chains (*white*) and light chains (*dark gray*) are speculative but modeled in part on that known for the outer arm of *Chlamydomonas* (11, 12).

equivalent to the  $\alpha$  heavy chain of the two-headed sea urchin outer arm.

#### ***Predominance of $\beta$ /IC1 Subunit's Activity in the *In Vitro* Motility Assay***

The fact that the intact arm and the  $\alpha$  subunit can form structural and rigor bonds in solution raises the question of why these properties were not observed when the same particles were adsorbed to glass (16). The simplest and most likely explanation is that the  $\alpha$  subunit, alone or as part of the intact arm, becomes stuck down to and possibly denatured on the glass surface (Fig. 6). In the case of the intact arm, only the  $\beta$ /IC1 subunit then would be free to interact with the microtubules, so that the observed properties would be those of that subunit. A precedent for regular orientation of dynein upon adsorption to a surface is found in the binding of *Chlamydomonas* outer arm dynein to mica (4), although a regular orientation was not observed for sea urchin outer arm dynein bound to mica (22).

#### ***Structural Binding of Dynein to Microtubules***

Our conclusion that the  $\alpha$  subunit is involved in structural binding to microtubules is in agreement with the earlier observation that partial proteolysis of the  $\alpha$  heavy chain is correlated with the ability of the outer arm of sea urchin sperm to be solubilized by only 0.1 M NaCl in the presence of ATP (1). However, results with *Chlamydomonas* suggest that the  $\alpha$  heavy chain cannot be the only dynein polypeptide involved in structural binding, at least in that organism: (a) a mutant of *Chlamydomonas* has recently been identified that lacks the  $\alpha$  subunit yet assembles the  $\beta$  and  $\gamma$  subunits into a truncated outer arm (19); (b) the 78-kD intermediate chain of the *Chlamydomonas* outer arm dynein is in direct contact

with  $\alpha$  tubulin in the axoneme, suggesting that it plays a role in binding the arm to the A-tubule of the outer doublet (13); and (c) both the  $\alpha\beta$  dimer and the  $\gamma$  subunit must be present for either particle to rebind to axonemes stripped of their arms (Fay, R. B., and G. B. Witman. 1977. *J. Cell Biol.* 75:286 abstract), suggesting either that both particles contain binding sites with relatively low affinities for microtubules, or that interaction between the particles is necessary to unmask the binding site or stabilize binding. Further studies will be necessary to determine if some other polypeptide of sea urchin outer arm dynein has microtubule-binding properties not revealed by our studies, or whether the sea urchin  $\alpha$  heavy chain has assumed a binding function that is the property of a different dynein polypeptide in *Chlamydomonas*.

Although the purified outer arm dynein assembled in patches along microtubules, such cooperativity was not observed for the purified  $\alpha$  subunit. Therefore, the  $\alpha$  subunit apparently lacks a component necessary for interaction between adjacent dynein arms. This component may be a polypeptide of the IC/LC complex (see below), which is located at the base of the arm and is in a position to interact directly with the heads of the next most distal arm (11, 38). This might be tested by examination of the assembly properties of the purified  $\alpha$ / $\beta$ /IC1 complex (Fig. 1), which contains the two heavy chains but lacks ICs 2 and 3 and all of the light chains.

#### ***Structure and Behavior of Microtubule Bundles***

Pairs of parallel microtubules were commonly observed in both the presence and absence of added dynein. In the absence of added dynein, the pairs probably represented the branches of bifurcated microtubules that were sufficiently

rigid so that the branches only gradually diverged from each other. This is suggested by the observations that: (a) no bridges were ever observed between paired microtubules in the absence of added dynein; (b) the spacing between members of a pair varied greatly; (c) the walls of the microtubules in some pairs were in direct contact with each other. Although no unequivocal examples of bifurcation were seen in cross or longitudinal sections (however, see Fig. 5 C), S-shaped protofilament sheets and microtubules with protofilament hooks were observed which may have represented intermediate steps in microtubule bifurcation. Similar microtubule pairs are visible in previously published electron micrographs of preparations of microtubules assembled from purified brain tubulin (see e.g., Fig. 7 of reference 8), although to our knowledge they have not been noted by the investigators.

Pairs of microtubules observed in the presence of intact outer arm dynein differed from those seen in the absence of dynein in that they were cross-bridged by one or two rows of dynein arms, and members of a pair were always separated by a constant distance (54 nm center-to-center). It is probable that many of these paired microtubules also represented the branches of a bifurcated microtubule; in this case, the constant center-to-center spacing would have been imposed on the pair by the dynein cross-bridges. However, previously unassociated microtubules also were probably bound into pairs by dynein cross-bridges. In either case, it appears that once two microtubules are brought together by one row of dynein arms, it is thermodynamically favorable for a second row of arms to form between the same two microtubules.

More difficult to explain is the presence of sheets of microtubules in preparations bundled by crude dynein or purified outer arm dynein. In these sheets, arms usually were attached to opposite sides of a microtubule, suggesting that binding of an arm (or pair of arms) to one site on the microtubule wall perturbed the tubulin lattice so that binding of additional arms to the same microtubule was most likely to occur on the side of the microtubule opposite the initial binding site. A similar bundling of microtubules into large sheet-like arrays was induced by the isolated inner arm dynein II of *Chlamydomonas* (26). Binding of microtubule cross-bridges to opposite sides of microtubules to form microtubule sheets is observed in many microtubular structures in vivo, e.g., the axostyles of *Saccinobaculus* (39) and devescovinid flagellates (40), and the tubule rows and sleeves in *Tokophrya* (31). The fact that microtubule sheets were formed in our preparations indicates that such simple patterned arrays may self-assemble as the result of interactions between microtubules and cross-bridges, without the need for a microtubule organizing center to determine microtubule arrangement.

Microtubule bundles rarely fell apart by intermicrotubule sliding, even when held together by intact dynein that supported motility in gliding microtubule assays. This result may be explained by our ultrastructural observations that all of the microtubules in a bundle are oriented with the same polarity, and that many of the microtubules are linked by reciprocal dynein cross-bridges. Under these conditions, the dyneins in each of the two rows of arms between a pair of microtubules would push the opposing microtubule in the same direction, resulting in no net movement. Thus, the rare observations of intermicrotubule sliding probably involved a

microtubule connected to its neighbor by a single row of dynein arms.

Two additional factors may have limited microtubule sliding in our preparations. First, because the microtubules were usually bundled into ribbon-like arrays, those bundles which attached to the surface of the coverslip probably flattened out so that all microtubules in the bundle were in contact with the glass. Adhesion to the bare glass would have created an additional impediment to intermicrotubule sliding. Second, parallel microtubules originating from a bifurcated microtubule and still attached to that microtubule would not have been free to slide completely apart, although such microtubules presumably would be able to undergo repeated "looping out" from the bundle, as was observed for one microtubule in the present study, and as has been seen in reactivated, disintegrating axonemes (10).

### *An Intermediate Chain/Light Chain Complex*

Previous work showed that two of the three ICs of sea urchin sperm outer arm dynein remained associated with each other following low ionic strength dialysis (30). We report here that these two ICs copurify with five LCs as a discrete particle. Therefore, sea urchin outer arm dynein appears to contain an IC/LC complex which constitutes a significant proportion of the total mass and compositional complexity of the outer arm. Similar IC/LC complexes also have been observed in the outer arm dyneins of *Chlamydomonas* (11, 38) and trout sperm (12), indicating that such a complex is likely to be a general structural feature of the outer arm (38). The function of this complex is still unknown, although in *Chlamydomonas* it is located at the base of the dynein and is in direct contact with  $\alpha$  tubulin in the axoneme, suggesting that it may be involved in binding the arm to the outer doublet. In the experiments reported here, we did not observe direct interaction between the IC/LC complex and microtubules assembled in vitro from purified brain tubulin; however, this does not preclude the possibility that such interactions exist in situ.

We are grateful to Dr. S. P. Marchese-Ragona for providing the motile *Tetrahymena* outer arm dynein used in this work.

These studies were supported by National Institutes of Health grants GM30626 (G. B. Witman), GM12240 (A. G. Moss), HD20497 (W. S. Sale), and a grant from the Mellon Foundation.

Received for publication 20 February 1992 and in revised form 1 June 1992.

### *References*

1. Bell, C. W., and I. R. Gibbons. 1982. Structure of dynein 1 outer arm in sea urchin sperm flagella. II. Analysis by proteolytic cleavage. *J. Biol. Chem.* 257:516-522.
2. Binder, L. I., and J. L. Rosenbaum. 1978. The in vitro assembly of flagellar outer doublet tubulin. *J. Cell Biol.* 79:500-551.
3. Bradford, M. M. 1976. A rapid and sensitive method for the quantitation of microgram quantities of protein utilizing the principle of protein-dye binding. *Anal. Biochem.* 72:248-254.
4. Goodenough, U., and J. Heuser. 1984. Structural comparison of purified dynein proteins with *in situ* dynein arms. *J. Mol. Biol.* 180:1083-1118.
5. Haimo, L., B. Telzer, and J. L. Rosenbaum. 1979. Dynein binds to and crossbridges cytoplasmic microtubules. *Proc. Natl. Acad. Sci. USA.* 76:5759-5763.
6. Haimo, L. T., and J. L. Rosenbaum. 1981. Dynein binding to microtubules containing microtubule-associated proteins. *Cell Motility* 1:499-516.
7. Haimo, L., and R. B. Fenton. 1988. Interaction of *Chlamydomonas* dynein with tubulin. *Cell Motil. and Cytoskeleton.* 9:129-139.
8. Hitt, A. L., A. R. Cross, and R. C. Williams. 1990. Microtubule solutions

- display nematic liquid crystalline structure. *J. Biol. Chem.* 265:1639-1647.
9. Johnson, K. A. 1986. Preparation and properties of dynein from *Tetrahymena* cilia. *Methods Enzymol.* 134:306-317.
  10. Kamiya, R., and T. Okagaki. 1986. Cyclical bending of two outer-doublet microtubules in frayed axonemes of *Chlamydomonas*. *Cell Motil. and Cytoskeleton.* 6:580-585.
  11. King, S. M., and G. B. Witman. 1990. Localization of an intermediate chain of outer arm dynein by immunoelectron microscopy. *J. Biol. Chem.* 265:19807-19811.
  12. King, S. M., J.-L. Gatti, A. G. Moss, and G. B. Witman. 1990. Outer-arm dynein from trout spermatozoa: Substructural organization. *Cell Motil. and Cytoskeleton.* 16:266-278.
  13. King, S. M., C. G. Wilkerson, and G. B. Witman. 1991. The *M*, 78,000 intermediate chain of *Chlamydomonas* outer arm dynein interacts with  $\alpha$ -tubulin *in situ*. *J. Biol. Chem.* 266:8401-8407.
  14. Laemmli, U. K. 1970. Cleavage of structural proteins during the assembly of the head of bacteriophage T4. *Nature (Lond.)*. 227:680-685.
  15. Merrill, C. R., D. Goldman, S. A. Sedman, and M. H. Ebert. 1981. Ultrasensitive stain for proteins in polyacrylamide gels show regional variation in cerebrospinal fluid protein. *Science (Wash. DC)*. 211:1437-1438.
  16. Moss, A. G., J.-L. Gatti, and G. B. Witman. 1992. The motile  $\beta$ /IC1 subunit of sea urchin sperm outer arm dynein does not form a rigor bond. *J. Cell Biol.* 118:1177-1188.
  17. Paschal, B. M., S. M. King, A. G. Moss, C. A. Collins, R. B. Vallee, and G. B. Witman. 1987. Isolated flagellar outer arm dynein translocates brain microtubules *in vitro*. *Nature (Lond.)*. 330:672-674.
  18. Porter, M. E., and K. A. Johnson. 1983. Characterization of the ATP-sensitive binding of *Tetrahymena* 30S dynein to bovine brain microtubules. *J. Biol. Chem.* 258:6575-6581.
  19. Sakakibara, H., D. R. Mitchell, and R. Kamiya. 1991. A *Chlamydomonas* outer arm dynein mutant missing the  $\alpha$  heavy chain. *J. Cell Biol.* 113:615-622.
  20. Sale, W. S., and L. A. Fox. 1988. Isolated  $\beta$  heavy chain subunit of dynein translocates microtubules *in vitro*. *J. Cell Biol.* 107:1793-1798.
  21. Sale, W. S., and P. Satir. 1977. Direction of active sliding of microtubules in *Tetrahymena* cilia. *Proc. Natl. Acad. Sci. USA.* 74:2045-2049.
  22. Sale, W. S., U. W. Goodenough, and J. E. Heuser. 1985. The substructure of isolated and *in situ* outer dynein arms of sea urchin sperm flagella. *J. Cell Biol.* 101:1400-1412.
  23. Satir, P. 1982. Mechanisms and controls of microtubule sliding in cilia. *Symp. Soc. Exp. Biol.* 35:179-201.
  24. Shingyoji, C., A. Murakami, and K. Takahashi. 1977. Local reactivation of triton-extracted flagella by iontophoretic application of ATP. *Nature (Lond.)*. 265:269-270.
  25. Sleight, M. A., and D. I. Barlow. 1982. How are different ciliary beat patterns produced? *Symp. Soc. Exp. Biol.* 35:139-157.
  26. Smith, E. F., and W. S. Sale. 1991. Microtubule binding and translocation by inner arm subtype I1. *Cell Motil. and Cytoskeleton.* 18:258-268.
  27. Sugino, K., and Y. Naitoh. 1982. Simulated cross-bridge patterns corresponding to ciliary beating in *Paramecium*. *Nature (Lond.)*. 295:609-611.
  28. Summers, K. E., and I. R. Gibbons. 1971. Adenosine triphosphate-induced sliding of tubules in trypsin-treated flagella of sea-urchin sperm. *Proc. Natl. Acad. Sci. USA.* 68:3092-3096.
  29. Takahashi, M., and Y. Tonomura. 1978. Binding of 30S dynein with the b-tubule of the outer doublet of axonemes from *Tetrahymena pyriformis* and adenosine triphosphate-induced dissociation of the complex. *J. Biochem.* 84:1339-1355.
  30. Tang, W.-J. Y., C. W. Bell, W. S. Sale, and I. R. Gibbons. 1982. Structure of the dynein-1 outer arm in sea urchin sperm flagella. I. Analysis by separation of subunits. *J. Biol. Chem.* 257:508-515.
  31. Tucker, J. B. 1974. Microtubule arms and cytoplasmic streaming and microtubule bending and stretching of intertubule links in the feeding tentacle of the suction ciliate *Tokophrya*. *J. Cell Biol.* 62:424-437.
  32. Vallee, R. 1986. Reversible assembly purification of microtubules without assembly-promoting agents and further purification of tubulin, microtubule associated proteins, and MAP fragments. *Methods Enzymol.* 134:89-115.
  33. Warner, F. D. 1989. Preface. *In Cell Movement*. Vol. 1. The Dynein ATPases. Warner, F. D., P. Satir, and I. R. Gibbons, editors. A. R. Liss, Inc., New York. 337 pp.
  34. Witman, G. B. 1989. Composition and molecular organization of the dyneins. Chapter 2. *In Cell Movement*. Vol 1. The Dynein ATPases. F. D. Warner, P. Satir, and I. R. Gibbons, editors. Alan R. Liss, Inc., New York. 25-35.
  35. Witman, G. B. 1990. Introduction to cilia and flagella. Chapter 1. *In Structure and Function of Ciliary and Flagellar Surfaces*. Bloodgood, R. A., editor. Plenum Publishing Corp., New York. 1-30.
  36. Witman, G. B. 1992. Axonemal dyneins. *Curr. Opin. Cell Biol.* 4:74-79.
  37. Witman, G. B., and N. Minervini. 1982. Dynein arm conformation and mechanochemical transduction in the eukaryotic flagellum. *Soc. Exp. Biol. Symp.* 35:203-223.
  38. Witman, G. B., S. M. King, A. G. Moss, and C. G. Wilkerson. 1991. The intermediate chain/light chain complex: an important structural entity of outer arm dynein. *In Comparative Spermatology 20 Years After*. B. Bacetti, editor. Raven Press, New York.
  39. Woodrum, D. T., and R. W. Linck. 1980. Structural basis of motility in the microtubular axostyle: implications for cytoplasmic microtubule structure and function. *J. Cell Biol.* 87:404-414.
  40. Yamin, M. A., and S. L. Tamm. 1982. ATP reactivation of the rotary axostyle in termite flagellates: effects of dynein ATPase inhibitors. *J. Cell Biol.* 95:589-597.